JOURNAL OF VIROLOGY, Aug. 1992, p. 4940–4950
0022-538X/92/084940-11$02.00/0

Vol. 66, No. 8

Intermonomer Disulfide Bonds Impair the Fusion Activity of Influenza Virus Hemagglutinin

GEORGE W. KEMBLE,[1] DALE L. BODIAN,[1] JASON ROSÉ,[1] IAN A. WILSON,[2] AND JUDITH M. WHITE[1]*

Department of Pharmacology and Department of Biochemistry and Biophysics, University of California, San Francisco, California 94143-0450,[1] and Department of Molecular Biology, The Scripps Research Institute, La Jolla, California 92037[2]

Received 26 March 1992/Accepted 30 March 1992

At a low pH, the influenza virus hemagglutinin (HA) undergoes conformational changes that promote membrane fusion. While the critical role of fusion peptide release from the trimer interface has been demonstrated previously, the role of globular head dissociation in the overall fusion mechanism remains unclear. To investigate this question, we have analyzed in detail the fusion activity and low pH-induced conformational changes of a mutant, Cys-HA, in which the globular head domains are locked together by engineered intermonomer disulfide bonds (L. Godley, J. Pfeifer, D. Steinhauer, B. Ely, G. Shaw, R. Kaufmann, E. Suchanek, C. Pabo, J. J. Skehel, D. C. Wiley, and S. Wharton, Cell 68:635–645, 1992). In this paper, we show that Cys-HA expressed on the cell surface is predominantly a disulfide-bonded trimer. Cell surface Cys-HA is impaired in its membrane fusion activity, as demonstrated by both content-mixing and lipid-mixing fusion assays. It is also impaired in its ability to change conformation at a low pH, as assessed by proteinase K sensitivity. The fusion activity and low pH-induced conformational changes of cell surface Cys-HA are, however, restored to nearly wild-type levels upon reduction of the intermonomer disulfide bonds. By using a set of conformation-specific monoclonal and anti-peptide antibodies, we found that purified Cys-HA trimers are impaired in changes that occur in the globular head domain interface. In addition, changes that occur at a great distance from the engineered intermonomer disulfide bonds, notably release of the fusion peptides, are also impaired. Our results are discussed with respect to current views of the fusion-active conformation of the HA trimer.

Membrane fusion is an early and essential step mediating the entry of enveloped viruses into susceptible cells (34, 42). All enveloped viruses possess a specific protein that mediates this fusion event (34, 42). Of these integral membrane glycoproteins, the influenza virus hemagglutinin (HA) has been best characterized (44). HA is a trimer of three identical monomers. Each monomer is synthesized as a precursor, HA0, that is proteolytically processed into two disulfide-bonded polypeptide chains, HA1 and HA2. The ectodomain of this membrane protein has been described as having three domains, a globular head domain possessing receptor binding activity and major antigenic determinants, a hinge region, and, protruding from the membrane, a stem region where a sequence critical for fusion, the fusion peptide, is located (34, 42, 44, 48). In the normal replication cycle, the virion binds to the cell and enters by endocytosis. Upon encountering a low-pH endocytic environment, the HA changes conformation, the fusion peptides are released from the stem region of the trimer, and the viral and endocytic membranes fuse, releasing the viral ribonucleoprotein core into the cytoplasm (11, 13, 21, 26, 27, 30, 34, 38, 40, 42, 43, 49).

In a previous study, we characterized the low pH-induced conformational changes in the influenza virus HA (X:31 strain) by using a panel of anti-peptide antibodies (43). Our results suggested that the conformational changes occur in two major stages. In the first stage, changes occur in the stem region of the trimer, the most important being release of the fusion peptides from the trimer interface. In the second, the globular heads dissociate substantially from one another apparently by bending about the hinge region. Further characterization of the X:31 HA at 0°C and the HA from the Japan strain of influenza virus at 37°C has supported this two-stage conformational change model (5, 25, 33, 36). While prior work has demonstrated the importance of fusion peptide release during the first stage of the conformational change (19, 22), it has remained unclear whether the second stage of the conformational change is required for fusion or whether it represents a postfusion event (5, 25, 35, 36, 43).

To explore the role of dissociation of the globular head domains in the fusion reaction, we analyzed in detail the conformational changes and fusion activity of a mutant HA (Cys-HA) in which the heads of adjacent monomers were covalently joined via disulfide bonds (20). This mutant was shown to differ from wild-type HA in that, when it is exposed to a low pH, it does not change conformation nor does it induce syncytium formation or erythrocyte lysis (20). We have corroborated and extended these observations by using additional antibody probes against well-defined epitopes and two assays that directly measure membrane fusion. We present three major new findings. (i) The inability of Cys-HA to induce syncytium formation and erythrocyte lysis truly reflects its impaired membrane fusion function. (ii) A change which most likely represents partial dissociation of the globular head domains occurs during the first stage of the conformational change. (iii) The engineered intermonomer

* Corresponding author.

disulfide bonds in Cys-HA not only obstruct dissociation of the globular head domains but also restrict specific conformational changes that occur in the HA stem in response to low pH conditions, notably release of the fusion peptides.

MATERIALS AND METHODS

Antibodies. The site A mouse monoclonal antibody was a gift from John Skehel. It reacts equally well with properly folded neutral and low pH-treated HA (10, 48). The N1 and N2 mouse monoclonal antibodies, gifts of Ari Helenius, are specific for the neutral HA trimer (8, 36). These antibodies react with site B of the HA molecule at the tip of the globular head (36, 48). The interface mouse monoclonal antibody (H26D08) reacts with a peptide spanning amino acids 98 to 106 of the X:31 HA1 sequence. This epitope is completely buried within the trimer interface and is inaccessible to antibody molecules at a neutral pH (43, 47). However, the antibody does react with HA trimers that have been exposed to a low pH (43). Rabbit antisera against the fusion peptide (residues 1 to 29 of HA2) and loop peptide (14 to 52 of HA1) were gifts of Richard Lerner. These antisera preferentially recognize the acidified form of HA (43). The locations of the antibody epitopes used in this study are shown schematically on an HA monomer (see Fig. 6).

Cells and reagents. Cells expressing wild-type X:31 HA (wt-HA; H3 subtype, Wtm8005 cell line), Cys-HA (X:31 HA with the following substitutions: T-212→C and N-216→C), and parental CHO-DUKX cells were the generous gifts of Don Wiley (20). Cys-HA and Wtm8005 cells were maintained in G418 medium (minimal essential medium-alpha without nucleosides, 10% supplemented bovine calf serum [SCS], 2 mM glutamine, 100 U of penicillin per ml, 100 mg of streptomycin per ml, 600 μg of geneticin [GIBCO BRL, Gaithersburg, Md.] per ml, 0.3 μM methotrexate). CHO-DUKX cells were maintained in Ham's F-12 medium containing 10% SCS, 2 mM glutamine, 100 U of penicillin per ml, and 100 mg of streptomycin per ml. Unless otherwise indicated, all reagents for the maintenance of tissue culture cells were obtained from the UCSF Cell Culture Facility (San Francisco, Calif.) and all biochemical reagents were purchased from Sigma Chemical Co. (St. Louis, Mo.).

HA purification. Five T-175 flasks of cells expressing either wt-HA or Cys-HA were metabolically labeled with 0.5 mCi of ^{35}S Express Label (Dupont, NEN Research Products, Boston, Mass.) per flask for 18 h at 37°C in MEM Select-Amine lacking cysteine and methionine (GIBCO BRL). Unless otherwise indicated, the cells were incubated with 10 μg of tolylsulfonyl phenylalanyl chloromethyl ketone (TPCK)-trypsin per ml in RPMI 1640 for 8 min at room temperature (RT) to convert cell surface HA0 to HA1 and HA2. The cleavage reaction was quenched by the addition of 50 μg of soy trypsin inhibitor (STI) in RPMI 1640. The cells were removed from the dish by scraping into phosphate-buffered saline (PBS; 16 mM NaH_2PO_4, 2 mM Na_2HPO_4, 150 mM NaCl), collected by centrifugation at 115 × *g* for 5 min, and lysed for 30 min on ice in 1% Nonidet P-40 (NP-40)–0.1 M Tris, pH 7.5, containing a protease inhibitor cocktail (1 mM phenylmethylsulfonyl fluoride [PMSF], 1 μg of pepstatin A per ml, 2 μg of leupeptin per ml, 4 μg of aprotinin per ml, 10 μg of antipain per ml, 50 μg of benzamidine per ml, 10 μg of STI per ml, 0.5 mM iodoacetamide [IAA]). After centrifugation in a TLA100.3 rotor (Beckman Instruments, Inc., Fullerton, Calif.) at 70,000 × *g* for 30 min at 4°C, the detergent-soluble HA was purified by ricin affinity chromatography and sucrose gradient purification as described previously (43). Fractions corresponding to 9S trimers were pooled and used for immunoprecipitation analyses. The preparations were approximately 80% pure as determined by laser densitometry, the major contaminant being a 116-kDa polypeptide that does not cross-react with anti-HA antibodies (data not shown).

Immunoprecipitation. Samples of purified ^{35}S-wt-HA or ^{35}S-Cys-HA in MS buffer [0.13 M NaCl, 10 mM 2-(*N*-morpholino)ethanesulfonic acid (MES), pH 7.0] containing 0.1% NP-40 were treated at pH 5.0 and 37°C for the indicated times, reneutralized, and reacted with primary antibody for 2 h at RT. Final dilutions of antibodies were as follows: fusion peptide and loop, 1:5; N1 and interface, 1:100; N2, 1:25; and site A, 2.9 μg/ml. Protein-antibody complexes were precipitated for 1 h with 20 μl of protein A-agarose (Schleicher & Schuell, Inc., Keene, N.H.), washed twice with 0.5 M NaCl–10 mM Tris (pH 8.0), resuspended in 10% sodium dodecyl sulfate (SDS), and processed for scintillation counting.

Content-mixing fusion assay: delivery of erythrocyte-encapsulated lucifer yellow. A solution of 10 mg of lucifer yellow (K^+ salt; Molecular Probes, Eugene, Oreg.) per ml was incorporated into human erythrocytes as described previously (17), with a slight modification: the Hanks V buffer used to reseal the erythrocyte membranes consisted of 1.8 M NaCl–0.08 M KCl–0.02 M Na_2HPO_4. HA-expressing cells grown to 50 to 70% confluency on glass coverslips were rinsed twice in RPMI 1640 and treated with 0.2 mg of neuraminidase per ml containing either 10 μg of TPCK-trypsin per ml or 10 μg of STI per ml (HA0 controls) for 8 min at RT. This solution was removed, and 50 μg of STI per ml was added to inactivate the trypsin. Ham's F-12 medium–10% SCS was added, and the cells were returned to the 37°C incubator for 60 min to recover. Lucifer yellow-containing erythrocytes (1% suspension) were incubated with the cells for 20 min at RT, and the unbound erythrocytes were removed with three washes of RPMI 1640. A prewarmed solution of fusion buffer (10 mM HEPES [*N*-2-hydroxyethylpiperazine-*N'*-2-ethanesulfonic acid], 10 mM MES, 10 mM succinate, 120 mM NaCl, 2 mg of glucose per ml) at the indicated pH was added, and the cells were incubated in a 37°C water bath for 60 s. The fusion buffer was aspirated and replaced by Ham's F-12 medium–10% SCS, and the cells were returned to the 37°C incubator for 30 to 60 min. The coverslips were mounted, and photomicrographs were taken with an Olympus IMT-2 microscope. For dithiothreitol (DTT)-treated cells, the HA on the cell surface was reduced and alkylated (as described below) just prior to the binding of lucifer yellow-containing erythrocytes. Mock DTT-treated cells (−DTT) were subjected to alkylation only.

Lipid-mixing fusion assay: octadecylrhodamine (R_{18}) fluorescence dequenching. Confluent monolayers of CHO cells grown on 10-cm dishes were treated with trypsin and neuraminidase as described above, reduced and alkylated (as indicated elsewhere in the text), and then incubated with a 0.05% suspension of octadecylrhodamine (R_{18})-labeled erythrocytes prepared as described previously (24). The erythrocytes were bound for 10 min at RT, and the unbound cells were removed by six washes with RPMI 1640. The erythrocyte-CHO complexes were then rinsed twice with PBS–0.5 mM EGTA [ethylene glycol-bis(β-aminoethyl-ether)-*N,N,N',N'*-tetraacetic acid]–0.5 mM EDTA and removed from the tissue culture dish by gentle pipetting. The cells were placed in fusion buffer, pH 7.0, collected by centrifugation at 115 × *g* for 5 min at RT, resuspended in 0.5

ml of fusion buffer, pH 7.0, and placed on ice until further use.

An aliquot of the erythrocyte-CHO complexes was placed in a thermostatted cuvette containing 3 ml of 37°C fusion buffer, pH 7.0. Fluorescence measurements were made on an LS-5B fluorimeter equipped with a magnetic stirrer (Perkin-Elmer, San José, Calif.) by using an excitation wavelength of 560 nm and an emission wavelength of 590 nm. Fluorescence values were collected every 1.5 s with a Macintosh II computer (Apple Computer, Cupertino, Calif.) and VersaTerm Pro 3.1 communication software. After the collection of baseline values for 2 min, fusion was initiated by injecting a predetermined amount of 1 N acetic acid into the sample to bring the pH to 5.2. Fluorescence values were collected for an additional 3 min. The sample was then removed, and the cells were lysed by the addition of 160 μl of 10% NP-40 and incubated for 5 to 16 h at RT to obtain the amount of fluorescence at an infinite dilution ($F_{NP\text{-}40}$). The last 20 baseline values were averaged to obtain the baseline fluorescence (F_0), and the percent fluorescence dequenching (FDQ) was determined as follows:

$$\% \text{ FDQ} = [(F_t - F_0)/(F_{NP\text{-}40} - F_0)] \times 100$$

where F_t equals the fluorescence value at the time indicated. Two aliquots from each sample were independently monitored for the percent FDQ for 3 min postacidification, and the measurements were averaged. The highest average standard error for any of the sets did not exceed 4.5% FDQ. The maximal rate of the reaction (expressed as percent FDQ per minute) was obtained from the slope of the best-fit line through the linear portion of the curve that displayed the most rapid percent FDQ.

Reduction and alkylation of HA on the cell surface. Intact cells were rinsed twice with Tris-buffered saline (TBS) (50 mM Tris, 120 mM NaCl [pH 8.0]) and incubated in TBS alone or with the indicated amount of DTT in TBS for 10 min at RT. The DTT solution was removed, and the cells were rinsed once with TBS and incubated for an additional 15 min in 0.15 M IAA in TBS. The IAA was removed, and the cells were rinsed twice with RPMI 1640 before further processing.

Cell surface biotinylation and immunoprecipitation. Cells grown to confluency in 10-cm dishes were treated with trypsin, reduced with the indicated amount of DTT, and alkylated with IAA as described above. The cells were then removed from the dish with PBS–0.5 mM EGTA–0.5 mM EDTA and placed in PBS, pH 7.8. After centrifugation at 115 × *g* for 5 min at RT, cell surface proteins were labeled in 1 ml of PBS–1 mg of immunopure NHS-LC-biotin (Pierce Biochemicals, Rockford, Ill.) pH 7.8, per ml for 45 min at 4°C, and the reaction was quenched by the addition of 10 ml of PBS–50 mM glycine (pH 7.8) for 10 min at 4°C. The cells were collected by centrifugation, washed twice in PBS, and lysed in 0.5 ml of lysis buffer (1% NP-40, 50 mM HEPES, protease inhibitor cocktail [pH 7.2]). The lysate was centrifuged at 15,000 × *g* in an Eppendorf microcentrifuge at 4°C for 20 min, and 100 μg of soluble protein, determined by fluorescamine assay (37), was incubated with 1.5 μg of the site A monoclonal antibody for 60 min at RT. The antibody-HA complexes were precipitated with protein A-agarose for 60 min at RT and washed extensively as described previously (23). The immunocomplexes were suspended in loading buffer (62.5 mM Tris [pH 7.5], 2% SDS, 7.5% sucrose, 0.5 mM EDTA, 0.005% bromophenol blue), heated to 95°C for 5 min, and separated on a nonreducing SDS–8% polyacrylamide gel. The proteins were transferred to nitrocellulose; blocked with PBS, 1% skim milk, 10% glycerol, 3% bovine serum albumin, 1 M glucose, and 0.5% Tween 20; and probed with 10 μCi of [^{125}I]streptavidin (gift of Sam Green) in PBS–0.5% Tween 20 for 60 min at RT. The filters were washed three times in PBS–0.5% Tween 20, air dried, and subjected to autoradiography by using Hyperfilm (Amersham, Arlington Heights, Ill.) and phosphorimage analysis by using a PhosphorImager workstation (Molecular Dynamics, Sunnyvale, Calif.).

Proteinase K digestion assay. Following mild trypsinization (to cleave HA0), reduction, alkylation, and biotinylation as described above, the cells were washed once in MES-saline (30 mM MES, 100 mM NaCl [pH 7.0]). Aliquots of the intact cells were incubated in 1 to 2 ml of MES-saline at the indicated pH for 15 min at 37°C. The buffer was neutralized by the addition of a predetermined amount of 1 M Tris base, and the cells were washed twice with 5 to 10 volumes of MES-saline, pH 7.0, lysed in lysis buffer, and centrifuged at 15,000 × *g* in an Eppendorf microcentrifuge for 20 min at 4°C. Approximately 145 μg of each lysate, determined by a fluorescamine assay (37), was adjusted to 0.5 ml with lysis buffer and digested by the addition of 50 μl of 55 mM $CaCl_2$–2 mg of proteinase K per ml for 30 min at 37°C. After stopping the digestion by the addition of PMSF and bovine serum albumin (to final concentrations of 5 mM and 50 μg/ml, respectively), HA was precipitated by adding 1.5 μg of the site A monoclonal antibody and protein A-agarose. After extensive washing (23) with buffers containing 1 mM PMSF, the immunoprecipitates were resuspended in SDS sample buffer containing 100 mM DTT and 2 mM PMSF, heated at 95°C for 5 min, and separated by SDS–PAGE (10% polyacrylamide). The proteins were transferred to nitrocellulose and probed with [^{125}I]streptavidin as described above.

Computer modeling of HA. The ribbon drawing of HA was produced by using the MidasPlus software system from the Computer Graphics Laboratory, University of California, San Francisco (18), and displayed on an Iris 4D/80GT workstation (Silicon Graphics, Mountain View, Calif.). Coordinates of HA are from entry 2hmg (39) in the Brookhaven protein data bank (1, 3).

RESULTS

Fusion activity of Cys-HA and wt-HA before and after reduction. We assessed the membrane fusion potential of Cys-HA by using two independent membrane fusion assays, one that monitors content mixing (14, 32) and a second that measures lipid mixing (24). Before analyzing the fusion activity of Cys-HA-expressing cells, however, we characterized two parameters that affect fusion, the amount of Cys-HA on the cell surface and its ability to be proteolytically activated (15, 42, 44). Cys-HA- and wt-HA-expressing cells express the precursor form of HA, HA0, on their cell surface; HA0 must be proteolytically processed into two disulfide polypeptide chains, HA1 and HA2, in order to be fusion competent (42, 48). In order both to quantitate the expression and to assess the proteolytic processing of cell surface Cys-HA and wt-HA, cells were metabolically labeled for 16 h with ^{35}S, mildly trypsinized, and analyzed for HA0, HA1, and HA2 species (Fig. 1) (19). Phosphorimage analysis of the SDS gel revealed that approximately 65% of the Cys-HA expressed in the CHO cells was on the cell surface. Nearly all of the (biotinylated) cell surface Cys-HA was capable of being processed into its disulfide-linked Cys-HA1 and Cys-HA2 polypeptide chains by the addition of exogenous trypsin (Fig. 1; data not shown). In contrast, over 95% of the wt-HA was expressed on the cell surface

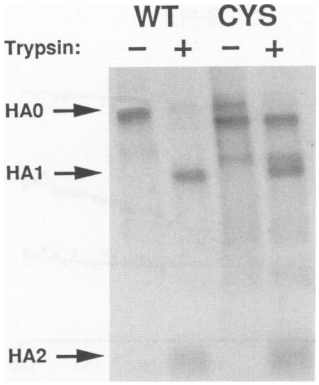

FIG. 1. Expression of HA1 and HA2 polypeptide chains on the surface of both wt-HA- and Cys-HA-expressing cells. Cells expressing either wt-HA or Cys-HA were incubated with 0.25 mCi of ^{35}S Express Label for 16 h, treated with 10 μg of trypsin per ml (lanes +) or STI (lanes −) for 10 min at RT, and lysed. Approximately 10^8 cpm of each sample was incubated with the site A antibody and precipitated. Immunocomplexes were resolved by reducing SDS-PAGE (10% polyacrylamide) and subjected to both autoradiography and phosphorimage analysis.

and properly processed (Fig. 1). However, since Cys-HA-expressing cells appeared to have made more total cellular HA than did wt-HA-expressing cells, the amounts of processed Cys-HA and wt-HA on the cell surface were equivalent (Fig. 1). Because the cell surface densities of processed Cys-HA and wt-HA are similar, direct comparisons of the fusion capacity of Cys-HA- and wt-HA-expressing cells can be made.

We first compared the fusion activity of Cys-HA and wt-HA by using a content-mixing assay. For this assay, we used erythrocytes loaded with lucifer yellow to determine whether the contents of bound erythrocytes could be delivered to HA-expressing cells after exposure to fusion-inducing conditions (14, 32). Lucifer yellow-containing erythrocytes were bound to HA-expressing cells, incubated in pH 5.2 fusion buffer for 60 s, and then returned to growth medium. After a further incubation for 30 min, the cells were observed with a fluorescence microscope. The cytoplasm of wt-HA-expressing cells became filled with lucifer yellow (Fig. 2A). However, very little cytoplasmic fluorescence was seen in Cys-HA-expressing cells; the lucifer yellow was confined predominantly to the bound erythrocytes (Fig. 2B). When Cys-HA cells were subjected to reduction and alkylation prior to the erythrocyte delivery protocol, lucifer yellow was visible in the cytoplasm of the majority of the cells (Fig. 2D). As expected, both proteolytic activation of wt-HA0 and Cys-HA0 and low pH treatment were required

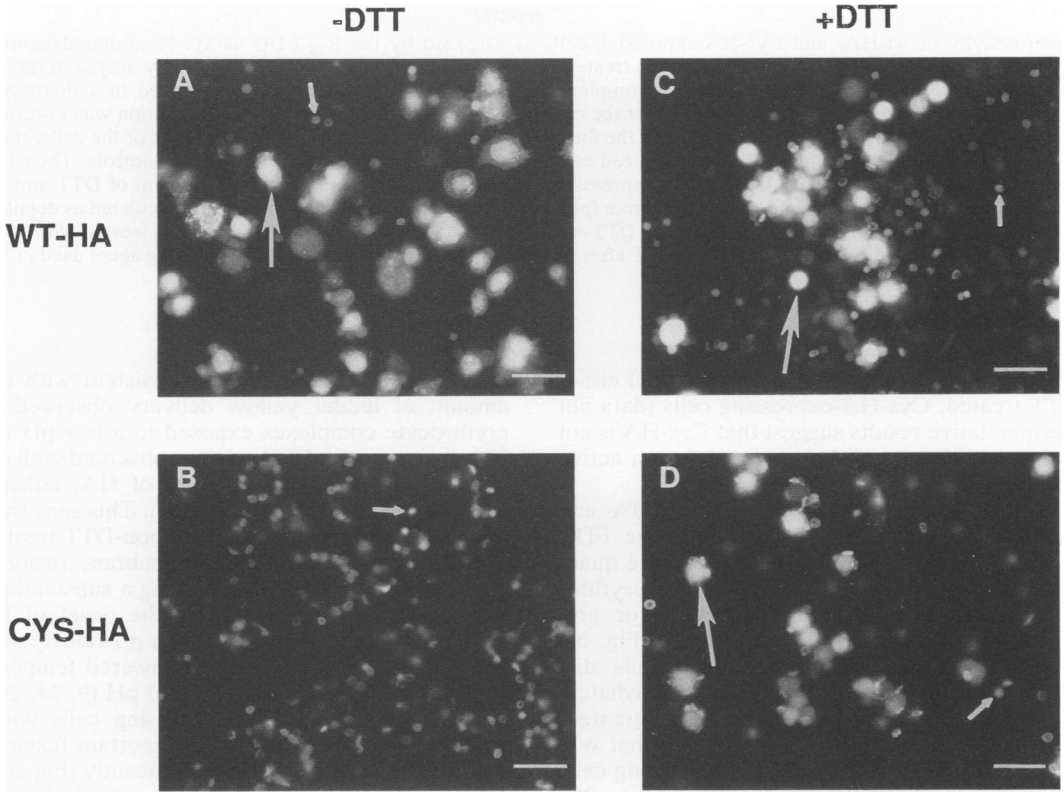

FIG. 2. Fusion activity of wt-HA- and Cys-HA-expressing cells assessed by the delivery of erythrocyte contents. Cells expressing either wt-HA (A and C) or Cys-HA (B and D) were either untreated (−DTT) (A and B) or reduced with 12 mM DTT and alkylated (+DTT) (C and D), as described in Materials and Methods. Erythrocytes containing lucifer yellow were bound to the cells, and the pH was lowered to 5.2 for 60 s at 37°C. The cells were returned to the medium at a neutral pH and incubated for 30 min at 37°C before mounting and photography. The small arrows mark bound lucifer yellow-containing erythrocytes, and the large arrows indicate HA-expressing cells that have taken up lucifer yellow after fusion. The more-rounded morphology of the wt-HA- and Cys-HA-expressing cells in panels C and D was due to the reduction and alkylation. Bar = 40 μm.

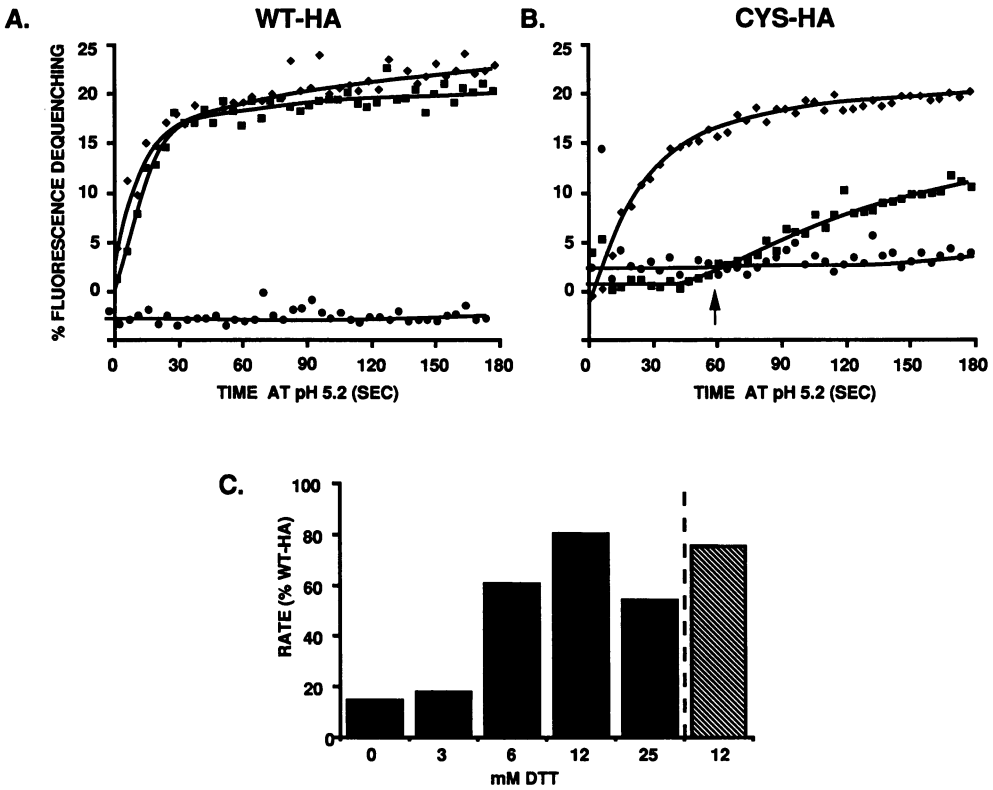

FIG. 3. Fusion activity of wt-HA- and Cys-HA-expressing cells as assessed by the R_{18} FDQ assay. Neuraminidase-treated, trypsin-activated cells expressing either wt-HA (A) or Cys-HA (B) treated with 12 mM DTT and alkylated (◆) or only alkylated (■) were bound to erythrocytes labeled with R_{18}, and the erythrocyte-cell complexes were removed from the dish and placed in a thermostatted cuvette containing 37°C fusion buffer (pH 7.0) in a fluorimeter. After the collection of baseline data, the pH of the solution was lowered to 5.2 by the injection of a predetermined amount of 1 N acetic acid and the fluorescence values were measured. After lysis of the cells, the percent FDQ was calculated and plotted with respect to time. Untrypsinized cells expressing HA0 (●) served as negative controls. The 60-s time point is indicated (↑) for comparison with Fig. 2B. (C) Cys-HA-expressing cells (■) treated with the indicated amount of DTT and alkylated were subjected to the procedure outlined above and the maximal rate (percent FDQ per min) for each sample was calculated as detailed in Materials and Methods and compared with the maximal rate for non-DTT-treated wt-HA cells. Wt-HA-expressing cells treated with 12 mM DTT (▧) are also shown. Since the intact cells were treated with DTT after trypsinization, the concentrations of reducing agent used in this study were significantly lower than that used by Godley et al. (20).

to detect significant fluorescence in the cytoplasm of either wt-HA- or DTT-treated, Cys-HA-expressing cells (data not shown). These qualitative results suggest that Cys-HA is not fusion competent but that it can be rendered fusion active after treatment with DTT.

We next compared the fusion competence of wt-HA- and Cys-HA-expressing cells by using a more-sensitive FDQ lipid-mixing assay. This assay allowed us to compare quantitatively the time course of fusion of R_{18}-labeled erythrocytes and HA-expressing cells, either untreated or pretreated with various amounts of DTT. As seen in Fig. 3A (squares), non-DTT-treated, wt-HA-expressing cells displayed a rapid initial rate of FDQ that began immediately after lowering the pH. In sharp contrast, non-DTT-treated, Cys-HA-expressing cells fused at a maximal rate that was only 15% that of non-DTT-treated, wt-HA-expressing cells and only following a substantial lag (~40 s) (Fig. 3B, squares). The extent of fusion with non-DTT-treated, Cys-HA-expressing cells reached 55% of wt levels after 3 min of acidification, while fusion mediated by non-DTT-treated, wt-HA-expressing cells plateaued within 1 min (Fig. 3A and B). The negligible amount of lipid mixing observed with non-DTT-treated, Cys-HA-expressing cells at 60 s postacidification (Fig. 3B, arrow) is consistent with the negligible amount of lucifer yellow delivery observed in Cys-HA–erythrocyte complexes exposed to a low pH for 60 s (Fig. 2B). As expected, FDQ was not observed with cells expressing the nonfusogenic precursor of HA, either wt-HA0 or Cys-HA0 (Fig. 3A and B, circles). This sensitive membrane fusion assay demonstrated that non-DTT-treated, Cys-HA-expressing cells do mediate membrane fusion, albeit at a greatly reduced rate and following a substantially increased lag phase. Lag phases before the onset of HA-mediated membrane fusion have been seen previously under suboptimal fusion conditions such as lowered temperature, lower HA surface density, and elevated pH (9, 24, 28, 32, 36).

Treatment of Cys-HA-expressing cells with increasing amounts of DTT affected two important fusion parameters. The rate of fusion increased significantly (Fig. 3B, diamonds; Fig. 3C). The lag phase before the onset of fusion (Fig. 3B, squares) was abolished (Fig. 3B, diamonds). For Cys-HA-expressing cells treated with 12 mM DTT, the maximal rate of fusion was fivefold greater than for the non-DTT-treated Cys-HA cells (Fig. 3C). This rate of fusion was approximately 80% that of the non-DTT-treated wt-HA controls and equivalent to that of wt-HA-expressing cells treated with 12

mM DTT (Fig. 3C). Treatment with higher concentrations of DTT (≥25 mM) led to a decrease in the rate of fusion for both wt-HA and Cys-HA (Fig. 3C; data not shown). The results of both the content-mixing (Fig. 2) and lipid-mixing (Fig. 3) fusion assays indicate that DTT treatment of Cys-HA-expressing cells restores the fusion competence of cell surface Cys-HA to wt levels.

Oligomeric forms of cell surface Cys-HA and wt-HA before and after reduction. The results of the fusion experiments suggest that the engineered intermonomer disulfide bonds in cell surface Cys-HA are reduced by DTT treatment. To test this hypothesis, we performed experiments to analyze the effects of DTT treatment on HA present on the surface of intact wt-HA- and Cys-HA-expressing cells. Biotinylated cell surface HA was monitored on nonreducing SDS gels (Fig. 4A) and quantitated by phosphorimage analysis (Fig. 4B). As shown in Fig. 4A, non-DTT-treated wt-HA migrated predominantly as the monomer, although other forms including trimer, dimer, HA1, and HA2 are visible. Treatment with increasing amounts of DTT increased the abundance of HA1 and HA2 while simultaneously decreasing the proportion of the monomer and higher oligomers (Fig. 4A, lanes 2 to 6). In contrast, approximately 90% of the non-DTT-treated Cys-HA migrated as the trimer, with only a small amount of monomer detectable (Fig. 4A, lane 8, and 4B). Treatment with increasing concentrations of DTT decreased the amount of the trimer and concomitantly increased the amount of the monomer, HA1, and HA2 visible on these gels (Fig. 4A, lanes 9 to 13). Virtually no trimer remained after treatment with 75 mM DTT (Fig. 4B). After exposure to 12 mM DTT (Fig. 4B, arrow), the concentration found optimal to enhance the fusion rate (Fig. 3C), approximately 50% of the cell surface Cys-HA migrated as trimer. While treatment with higher concentrations of DTT resulted in even lower proportions of the trimer and higher proportions of the monomer bands, there was also a concomitant increase in the amount of HA1 and HA2 seen on nonreducing gels (Fig. 4) and a concomitant reduction in fusion activity (Fig. 3C; data not shown). Presumably, the appearance of the HA1 and HA2 bands on these nonreducing gels indicates that the HA1-HA2 disulfide bond, and most likely other intrasubunit disulfide bonds, has been broken. This analysis indicated that approximately 90% of the cell surface Cys-HA is cross-linked by engineered intermonomeric disulfide bonds that can be reduced by the treatment of intact cells with DTT.

Low pH-induced conformational changes of cell surface Cys-HA and wt-HA before and after reduction. The HA protein undergoes a characteristic conformational change upon exposure to low pH conditions. One hallmark of this change is that the protein, normally resistant to the degradative action of proteinase K, becomes susceptible to digestion. This property is acquired during the first stage of the conformational change (25, 41). We therefore analyzed the proteinase K sensitivity of neutral and low pH-treated cell surface Cys-HA both before and after reduction. Intact cells expressing wt-HA or Cys-HA were biotinylated, treated at a low pH, neutralized, and lysed in nonionic detergent, and the lysates were digested with proteinase K. As seen in Fig. 5, low pH-treated wt-HA was susceptible to proteinase K digestion either with or without prior DTT treatment. However, the majority of low pH-treated Cys-HA was resistant to digestion with proteinase K. This effect was partially reversed by pretreatment with 12 mM DTT. Phosphorimage analysis indicated that 25% of the non-DTT (but low pH)-treated Cys-HA was sensitive to digestion, compared with

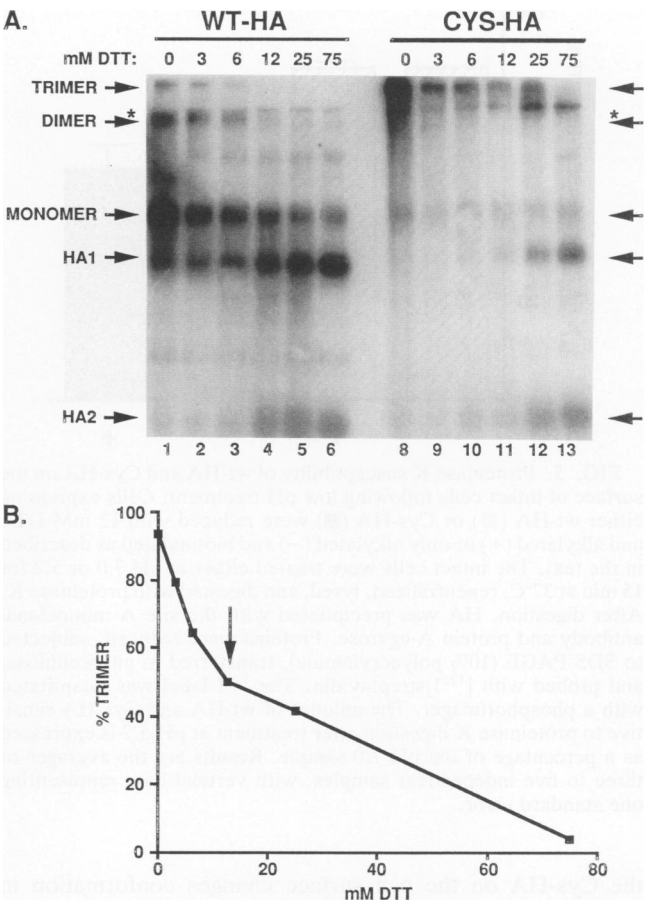

FIG. 4. Reduction of wt-HA and Cys-HA on the surfaces of intact cells. Intact wt-HA- and Cys-HA-expressing cells were surface labeled with NHS-LC-biotin, treated with the indicated amounts of DTT, alkylated with IAA, and lysed with NP-40. One hundred micrograms of protein was precipitated with the site A monoclonal antibody and protein A-agarose. The antigen-antibody complexes were denatured in nonreducing sample buffer, separated by nonreducing SDS-PAGE (8% polyacrylamide), transferred to nitrocellulose, and probed with [^{125}I]streptavidin. (A) Autoradiogram of the cell surface wt-HA (lanes 1 to 6) and Cys-HA (lanes 7 to 12) from cells treated with various concentrations of DTT (indicated above each lane). Arrows on the left and the right mark the positions of the HA trimer, dimer, and monomer and the HA1 and HA2 subunits. A band that is present on non-HA-expressing CHO-DUKX cells that cross-reacts with the site A monoclonal antibody and migrates slightly more slowly than the HA dimer is indicated (*). The relatively low level of biotinylated Cys-HA detected is presumably due to an inefficiency in the detection system. When equivalent samples were reduced, comparable amounts of Cys-HA and wt-HA were detected (data not shown). (B) The bands were quantitated by phosphorimage analysis. The amount of Cys-HA trimer is expressed as a percentage of all Cys-HA forms (←) in each lane. The sample treated with 12 mM DTT, the concentration found optimal to restore fusion competence, is also shown (↓).

90% for wt-HA. Treatment with 12 mM DTT (the concentration found optimal to enhance the fusion rate; Fig. 3C) augmented to 60% the amount of low pH-treated Cys-HA sensitive to proteinase K. The results of this assay suggest that approximately 25% of the Cys-HA on the surface of non-DTT-treated cells is able to change conformation and that after reduction with 12 mM DTT approximately 60% of

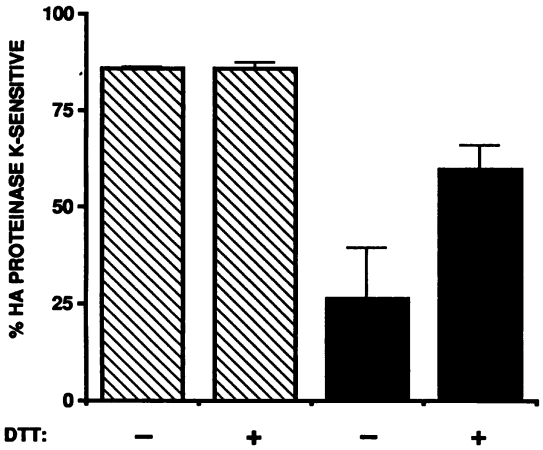

FIG. 5. Proteinase K susceptibility of wt-HA and Cys-HA on the surface of intact cells following low pH treatment. Cells expressing either wt-HA (▨) or Cys-HA (■) were reduced with 12 mM DTT and alkylated (+) or only alkylated (−) and biotinylated as described in the text. The intact cells were treated either at pH 7.0 or 5.2 for 15 min at 37°C, reneutralized, lysed, and digested with proteinase K. After digestion, HA was precipitated with the site A monoclonal antibody and protein A-agarose. Proteins were reduced, subjected to SDS-PAGE (10% polyacrylamide), transferred to nitrocellulose, and probed with [^{125}I]streptavidin. The ^{125}I label was quantitated with a phosphorimager. The amount of wt-HA and Cys-HA sensitive to proteinase K digestion after treatment at pH 5.2 is expressed as a percentage of the pH 7.0 sample. Results are the averages of three to five independent samples, with vertical bars representing one standard error.

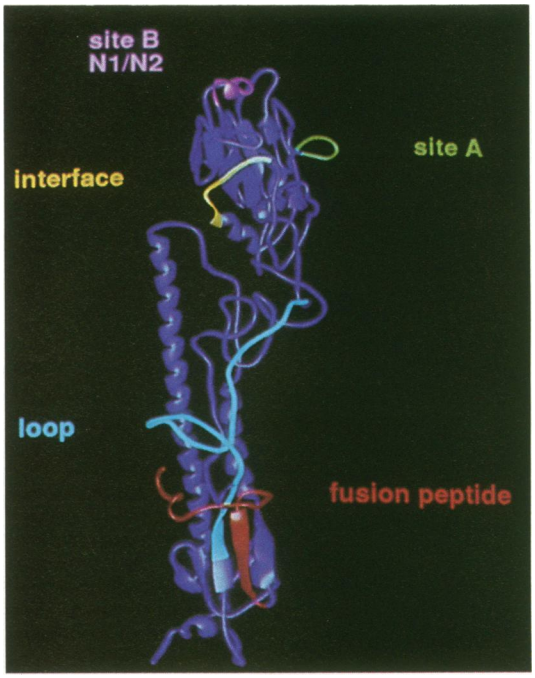

FIG. 6. Ribbon drawing of the HA monomer (dark blue), showing locations of epitopes, as probed with conformation-specific antibodies, as follows: site A, green; site B (N1/N2), magenta; fusion peptide, red; interface, yellow; loop, cyan.

the Cys-HA on the cell surface changes conformation in response to a low pH.

Low pH-induced conformational changes in purified Cys-HA and wt-HA trimers. To characterize more precisely the ability of Cys-HA to undergo fusion-inducing conformational changes, purified, detergent solubilized ^{35}S-labeled wt-HA and Cys-HA trimers were compared for their ability to react with a set of conformation-specific antibodies before and after exposure to a low pH. The epitopes recognized by these probes are shown diagrammatically on a monomer of HA in Fig. 6. As shown previously (6, 36, 43) and in Table 1, exposure of wt-HA to a low pH resulted in its conversion to the low pH form, as evidenced by its acquisition of antibody reactivity to fusion peptide, loop, and interface epitopes, as well as its loss of reactivity with N1, a neutral pH, trimer-specific antibody (8). The conformational change as detected by binding of these antibodies was more modest in Cys-HA (Table 1). Overall, this analysis with four conformation-specific antibodies against defined epitopes indicated that non-DTT-treated Cys-HA is significantly impaired in its ability to undergo the low pH-induced conformational changes associated with wt-HA, even those that occur at a great distance, in the stem of the molecule.

To extend this analysis, we compared wt-HA and Cys-HA for the time course and extent of acquisition of reactivity to the anti-fusion peptide antibody and loss of reactivity to N2, another trimer-specific antibody. Low pH-treated wt-HA quickly acquired reactivity with the fusion peptide antiserum and concomitantly lost its reactivity with N2 (Fig. 7A). In contrast, although the time courses were similar, the extent of these conformational changes in Cys-HA was greatly reduced (Fig. 7B). Nevertheless, for both wt-HA and Cys-HA, a good correlation between the time courses and extents of fusion peptide exposure and loss of the neutral-specific epitope, N2, was observed. These results suggest that loss of the N2 epitope located at the tip of the globular head domain interface occurs concomitantly with exposure of the fusion peptide epitope, and, most importantly, when the globular head domains are physically joined, both of these changes are markedly and commensurately inhibited.

DISCUSSION

Membrane fusion is important for delivering the genome of an enveloped virus into a susceptible cell as well as for many aspects of a cell's normal function (34, 42, 45, 46). We and others have studied how the influenza virus HA medi-

TABLE 1. Comparison of antibody binding to wt-HA and Cys-HA[a]

Epitope	% Input counts precipitated					
	wt-HA			Cys-HA		
	pH 7	pH 5	Δ[b]	pH 7	pH 5	Δ
Fusion peptide	1	36	+35	1	10	+9
Loop	1	43	+42	1	7	+6
N1	44	1	−43	37	25	−12
Interface	0	10	+10	0	1	+1

[a] ^{35}S-labeled wt-HA and Cys-HA trimers were purified from cells and treated at the indicated pH for 5 (fusion peptide, loop, and N1) or 15 (interface) min at 37°C, reneutralized, and precipitated with the indicated antibody. The percentages of input counts precipitated are shown. Each entry is the average of two samples. This experiment was performed three separate times with similar results.

[b] Difference in percent counts per minute precipitated between pH 5- and pH 7-treated wt-HA or Cys-HA.

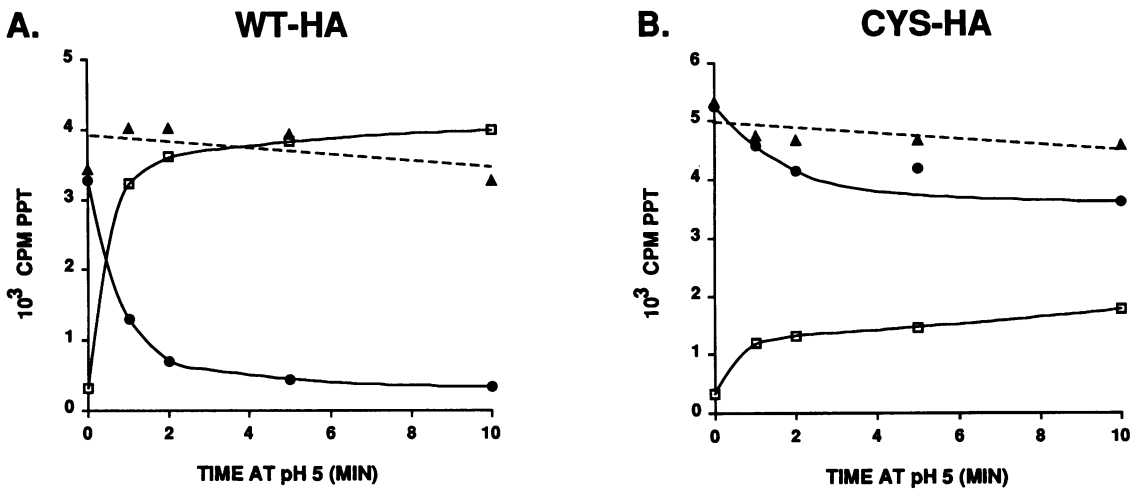

FIG. 7. Low pH-induced conformational changes in wt-HA and Cys-HA. ^{35}S-labeled wt-HA (A) or ^{35}S-labeled Cys-HA (B) were incubated at pH 5.0 for the indicated times and then reneutralized. The proteins were incubated with either the site A (▲), N2 (●), or fusion peptide (□) antibody for 2 h, and the protein-antibody complexes were precipitated with protein A-agarose, washed, and processed for scintillation counting as described in the test. The counts per minute precipitated (PPT) under these conditions are shown.

ates membrane fusion (for reviews, see references 2, 34, 42, and 44). Upon exposure to a low pH, the HA molecule retains its overall secondary structure but undergoes rearrangements altering its tertiary structure such that the fusion peptides are extruded from within the trimer stem and the heads separate substantially from one another, exposing epitopes within the interface of the globular head domains (11, 13, 21, 26, 27, 30, 34, 38, 40, 42, 43, 49). Both biochemical and genetic studies have demonstrated the critical role for the fusion peptides, and hence their release, in the fusion reaction (19, 22). However, the requirement for dissociation of the head domains has remained unclear. To understand more fully the role of globular head domain dissociation, we analyzed in detail the membrane fusion activity and conformational changes of a mutant, Cys-HA, in which the head groups were covalently cross-linked by engineered intermonomer disulfide bonds (20).

Fusion activity of Cys-HA-expressing cells is impaired. Cells that express Cys-HA do not make syncytia, and rosettes of Cys-HA polypeptides are compromised in their ability to mediate erythrocyte lysis (20). Although both of these activities are correlates, neither is a direct measure of membrane fusion activity, as shown by the following findings: (i) the replacement of glutamic acid with glycine (E-11→G) in the HA fusion peptide renders HA incapable of forming syncytia yet fully competent to mediate fusion with an erythrocyte at the same pH as that of a wt-HA (19); (ii) syncytium formation is highly dependent on the surface density of HA molecules (9, 15, 19); and (iii) membrane lysis can occur in the absence of membrane fusion (16, 31). Therefore, we used two independent membrane fusion assays to test whether Cys-HA in the plasma membrane of intact cells is truly impaired in its ability to induce membrane fusion. Delivery of both the contents and the membrane lipids of erythrocytes to Cys-HA-expressing cells following low-pH treatment was greatly impaired. Moreover, lipid mixing occurred only at a slow rate and after a substantial lag. The inhibition of Cys-HA functioning can be attributed to the engineered disulfide bonds, and not simply to the amino acid replacements T-212→C and N-216→C, since treatment of cell surface Cys-HA with 12 mM DTT restored the maximal fusion rate of Cys-HA to wt levels, abolished the lag phase before fusion, and accentuated the ability of Cys-HA to change conformation at a low pH (Fig. 2, 3, and 5).

At low pH, 10 to 25% of cell surface Cys-HA molecules change conformation. Cys-HA molecules present on the surface of intact cells are predominantly covalently linked trimers (Fig. 4). However, a percentage are not fully cross-linked by intermonomeric disulfide bonds. On nonreducing gels, approximately 10% of cell surface Cys-HA migrated as the monomeric species (Fig. 4). However, because noncovalently linked oligomers of wt-HA often do not migrate as monomeric species on nonreducing gels (Fig. 4, lane 1) (12), 10% is a lower estimate of the amount of noncovalently bonded cell surface Cys-HA. We also demonstrated that approximately 25% of both non-DTT-treated cell surface Cys-HA and purified Cys-HA trimers were able to undergo a pH-induced conformational change after exposure to a low pH (Fig. 5 and 7; and Table 1). These results suggest that a fraction of cell surface Cys-HA trimers change conformation when exposed to a low pH, most likely because they do not contain three intermonomer disulfide bonds.

Correlation between the membrane fusion activity and conformational changes of cell surface Cys-HA. Our collective results indicate that the engineered intermonomer disulfide bonds inhibit the conformational changes and fusion activity of Cys-HA. However, by using a sensitive and quantitative lipid-mixing assay, fusion was measured with Cys-HA-expressing cells. The rate of fusion was approximately 15% of that observed with wt-HA-expressing cells, and fusion was initiated only after a substantial lag phase. The fusion rate for Cys-HA-expressing cells correlates well with the estimate that 10 to 25% of the Cys-HA present on the cell surface is able to undergo a conformational change in response to low pH. (The extent of fusion between erythrocytes and non-DTT-treated, Cys-HA-expressing cells after 3 min at a low pH was 55% of the maximal extent attained by wt-HA-expressing cells at 1 min postacidification. However, fusion extent is not always a good comparative indicator of membrane fusion activity. When HA-mediated fusion occurs at a reduced rate because of suboptimal conditions such as an elevated pH, low temperature, and low HA surface

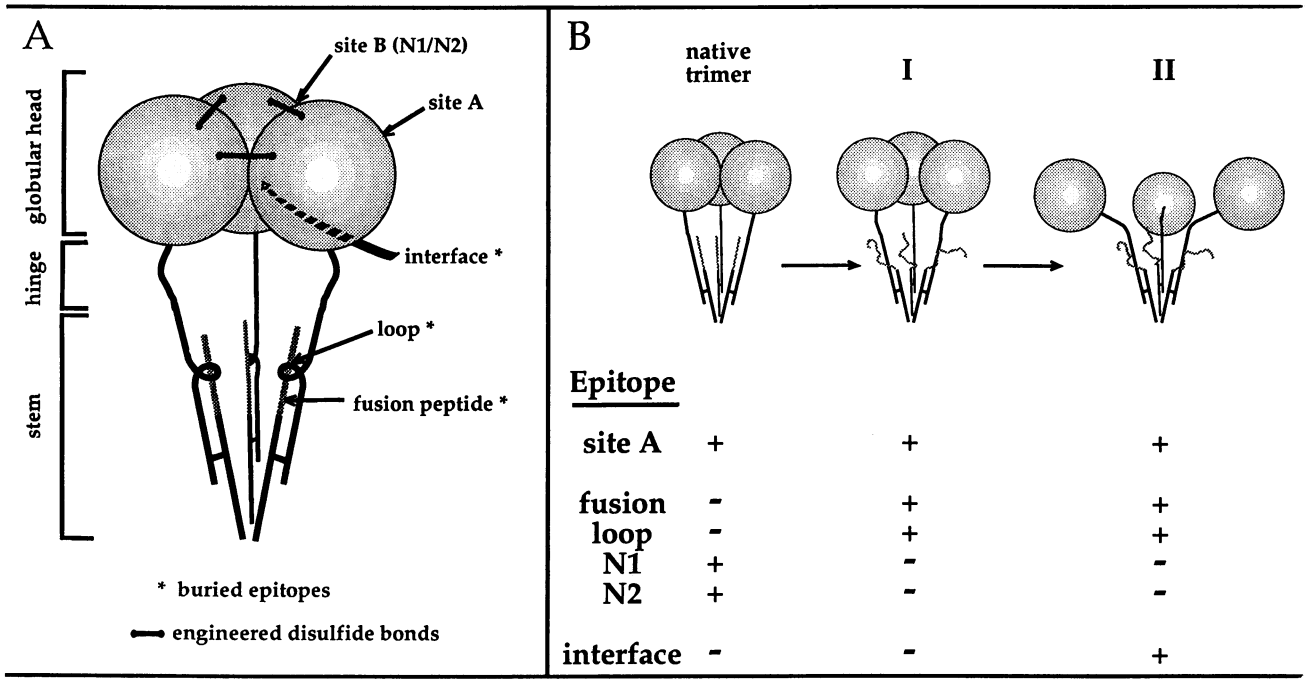

FIG. 8. Schematic representation of the native HA trimer and its low pH-induced conformational changes. (A) Representation of the HA trimer showing the three subdomains of the HA ectodomain (globular head, hinge, and stem), the locations of the epitopes probed in this study, and the disulfide bonds engineered into Cys-HA at residues HA1 212 and 216. (B) Depiction of our current model for low pH-induced conformational changes in HA. In stage I, the globular heads have partially dissociated from each other; the epitopes in the stem, the fusion peptide (dashed line or squiggle) and the loop peptide, have been exposed. In stage II, major dissociation of the globular head domains has occurred. Below, the presence (+) or absence (−) of a particular epitope is shown.

density, the extent of fusion often equals or surpasses that measured under optimal conditions [7, 9, 24, 36].)

There are three possible ways to explain the findings that non-DTT-treated, Cys-HA expressing cells display some fusion activity and conformational changes at low pH. (i) HA in which the globular head domains are fully disulfide bonded to one another has inherent, but significantly reduced, activity. In other words, conformational changes and fusion can occur, albeit at a greatly reduced rate, when the heads are completely locked together. (ii) Fully disulfide-bonded HA is totally impaired in its ability to change conformation and promote fusion; the low activity seen is due to Cys-HA molecules that are not fully cross-linked by intermonomer disulfide bonds. (iii) The answer could be a combination of the preceding two possibilities. Neither our results nor those presented by Godley et al. (20) rigorously distinguish between these possibilities. However, because of the correlation between the fusion rate (15%) and conformational changes (25%) of non-DTT-treated, Cys-HA-expressing cells with the amount of non-cross-linked Cys-HA trimer (≥10%) detected on the surface of these cells, we favor the second hypothesis.

Partial dissociation of the globular head domains occurs during the first stage of low pH-induced conformational change. Our previous work using conformation-specific anti-peptide antibodies demonstrated that HA changes conformation in two stages (43). The first stage is defined as those changes that occur in less than 60 s at 37°C. Marked changes occur in the stem region of HA during stage 1, including exposure of the loop, the C terminus of HA1, and fusion peptide epitopes (Fig. 6). Changes during the second stage (half-life, ~4 min) are characterized by exposure of peptide sequences located between the head groups, such as the interface epitope (Fig. 8, stage II). Biophysical measurements and electron microscopic observations suggest that, during the second stage of the conformational change, the head groups separate substantially from one another (30, 34, 43).

While comparing the ability of Cys-HA and wt-HA to undergo low pH-induced conformational changes, we discovered that a change in the globular head domains, as evidenced by the loss of the N1 and N2 epitopes, occurs during the first stage of the conformational change concomitant with fusion peptide exposure. The time courses of both antigenic changes were the same in both wt-HA and Cys-HA, and the extents of both of these changes were commensurately diminished in Cys-HA (Fig. 7). Since the N1 and N2 epitopes appear coincident with trimerization of the molecule (8) and since there are no gross secondary structural changes to HA after low-pH treatment (29, 30, 44), this change likely represents partial dissociation of the head domains. We therefore propose a refined model for the conformational change in HA in which partial dissociation of the globular head domains occurs during the first stage and major dissociation occurs during the second stage (Fig. 8).

Role of globular head domain dissociation in HA-mediated fusion. Two recent studies support the notion that major dissociation of the globular head domains, operationally defined here as the maximal separation of the globular head domains from one another (Fig. 8, stage II), is not required for fusion. With X:31 HA (an H3 subtype) at 0°C or Japan HA (an H2 subtype) at 37°C, the second stage of the conformational change appears to be inhibited, yet fusion proceeds (25, 33, 36). Also, the time course of fusion of X:31

virus (35) is faster than that of the second-stage changes (43). These findings do not, however, rule out the possibility that, as we suggest, partial separation of the globular head domains is required for fusion, at least for the X:31 strain. Partial dissociation of the globular head domains could be required to promote fusion peptide release, to expose other regions of HA involved in fusion, or to bring the fusing membranes closer together.

In apparent contrast with our present findings, a previous study demonstrated that at 0°C the fusion peptides of X:31 HA are exposed and the virus is able to mediate fusion (albeit at a greatly reduced rate and after a substantial lag) without irreversible dissociation of the globular head domains as monitored by the N1, N2, and interface antibodies (36). There are two ways to explain this minor paradox. First, the behavior of X:31 HA at 0°C may not accurately reflect the conformational changes needed to elicit fusion at the physiological temperature. Second, at 0°C and a low pH, partial dissociation of the globular head domains may be reversed upon reneutralization, unlike for HA exposed to a low pH at 37°C.

In conclusion, our results suggest that partial dissociation of the globular head domains is a prerequisite for the expression of the optimal membrane fusion activity of the X:31 HA. In addition to their relevance to the fusion mechanism of the influenza virus HA, our results speak to the design of fusion-inhibitory agents. Locking the monomers together in the HA globular head region has been proposed as a means of inhibiting the fusion activity of HA (20). We propose an inhibitor design strategy aimed directly at preventing fusion peptide release (4). Our present finding that fusion peptide exposure and membrane fusion activity are impaired in Cys-HA suggests that both strategies could have the same ultimate effect, preventing fusion peptide exposure and hence the fusion activity of influenza virus.

ACKNOWLEDGMENTS

We thank J. Skehel, A. Helenius, and R. Lerner for the gifts of antibodies and D. Wiley for the generous gift of the Cys-HA, Wtm8005, and CHO-DUKX cell lines used in this work. We also thank J. Skehel and D. Wiley for sharing a preprint of their recent publication (20).

This work was supported by a grant from NIH to J.M.W. (AI-22470) and, in part, by NIH grant AI-23498 (to I.A.W.).

REFERENCES

1. **Abola, E. E., F. C. Bernstein, S. H. Bryant, T. F. Koetzle, and J. Weng.** 1987. *In* F. H. Allen, G. Bergerhoff, and R. Seivers (ed.), Crystallographic databases—information content, software systems, scientific applications, p. 107–132. Data Commission of the International Union of Crystallography, Bonn.
2. **Bentz, J. (ed.).** 1991. Drug and anesthetic effects on membrane structure and function, p. 259–287. Wiley-Liss, New York.
3. **Bernstein, F. C., T. F. Koetzle, G. J. B. Williams, E. F. Meyer, Jr., M. C. Brice, J. R. Rodgers, O. Kennard, T. Shimanouchi, and M. Tasumi.** 1977. The protein data bank: a computer-based archival file for macromolecular structures. J. Mol. Biol. **112:** 535–542.
4. **Bodian, D., J. Stearns, J. White, and I. Kuntz.** Unpublished results.
5. **Bodian, D., and J. White.** 1992. Personal communication.
6. **Boulay, F., R. W. Doms, R. G. Webster, and A. Helenius.** 1988. Posttranslational oligomerization and cooperative acid activation of mixed influenza hemagglutinin trimers. J. Cell Biol. **106:**629–639.
7. **Clague, M. J., C. Schoch, and R. Blumenthal.** 1991. Delay time for influenza virus hemagglutinin-induced membrane fusion depends on hemagglutinin surface density. J. Virol. **65:**2402–2407.
8. **Copeland, C. S., K.-P. Zimmer, K. R. Wagner, G. A. Healey, I. Mellman, and A. Helenius.** 1988. Folding, trimerization, and transport are sequential events in the biogenesis of influenza virus hemagglutinin. Cell **53:**197–209.
9. **Danielli, T., and J. White.** 1992. Personal communication.
10. **Daniels, R. S., A. R. Douglas, J. J. Skehel, and D. C. Wiley.** 1983. Analyses of the antigenicity of influenza haemagglutinin at the pH optimum for virus-mediated membrane fusion. J. Gen. Virol. **64:**1657–1662.
11. **Daniels, R. S., J. C. Downie, A. J. Hay, M. Knossow, J. J. Skehel, M. L. Wang, and D. C. Wiley.** 1985. Fusion mutants of the influenza virus hemagglutinin glycoprotein. Cell **40:**431–439.
12. **Doms, R. W., and A. Helenius.** 1986. Quaternary structure of influenza virus hemagglutinin after acid treatment. J. Virol. **60:**833–839.
13. **Doms, R. W., A. Helenius, and J. White.** 1985. Membrane fusion activity of the influenza virus hemagglutinin. J. Biol. Chem. **260:**2973–2981.
14. **Doxsey, S., J. Sambrook, A. Helenius, and J. White.** 1985. An efficient method for introducing macromolecules into living cells. J. Cell Biol. **101:**19–27.
15. **Ellens, H., J. Bentz, D. Mason, F. Zhang, and J. M. White.** 1990. The fusion site of influenza hemagglutinin-expressing fibroblasts requires more than one hemagglutinin trimer. Biochemistry **29:**9697–9707.
16. **Ellens, H., J. Bentz, and F. C. Szoka.** 1986. Fusion of phosphatidylethanolamine-containing liposomes and mechanism of the La-HII phase transition. Biochemistry **25:**4141–4147.
17. **Ellens, H., S. Doxsey, J. S. Glenn, and J. M. White.** 1989. Delivery of macromolecules into cells expressing a viral membrane fusion protein. Methods Cell Biol. **31:**155–176.
18. **Ferrin, T. E., C. C. Huang, L. E. Jarvis, and R. Langridge.** 1988. The Midas display system. J. Mol. Graphics **6:**13–27.
19. **Gething, M.-J., R. W. Doms, D. York, and J. M. White.** 1986. Studies on the mechanism of membrane fusion: site-specific mutagenesis of the hemagglutinin of influenza virus. J. Cell Biol. **102:**11–23.
20. **Godley, L., J. Pfeifer, D. Steinhauer, B. Ely, G. Shaw, R. Kaufmann, E. Suchanek, C. Pabo, J. J. Skehel, D. C. Wiley, and S. Wharton.** 1992. Introduction of intersubunit disulfide bonds in the membrane-distal region of the influenza hemagglutinin abolishes membrane fusion activity. Cell **68:**635–645.
21. **Graves, P. N., J. L. Schulman, J. F. Young, and P. Palese.** 1983. Preparation of influenza virus subviral particles lacking the HA1 subunit of hemagglutinin: unmasking of cross-reactive HA2 determinants. Virology **126:**106–116.
22. **Harter, C., P. James, T. Bächi, G. Semenza, and J. Brunner.** 1989. Hydrophobic binding of the ectodomain of influenza hemagglutinin to membranes occurs through the "fusion peptide." J. Biol. Chem. **264:**6459–6464.
23. **Mellman, I. S., R. M. Steinman, J. C. Unkeless, and Z. A. Cohn.** 1980. Selective iodination and polypeptide composition of pinocytic vesicles. J. Cell Biol. **86:**712–722.
24. **Morris, S., D. Sarkar, J. White, and R. Blumenthal.** 1989. Kinetics of pH-dependent fusion between 3T3 fibroblasts expressing influenza hemagglutinin and red blood cells. Measurement by dequenching of fluorescence. J. Biol. Chem. **264:**3972–3978.
25. **Puri, A., F. P. Booy, R. W. Doms, J. M. White, and R. Blumenthal.** 1990. Conformational changes and fusion activity of influenza virus hemagglutinin of the H2 and H3 subtypes: effects of acid pretreatment. J. Virol. **64:**3824–3832.
26. **Ruigrok, R. W. H., A. Aitken, L. J. Calder, S. R. Martin, J. J. Skehel, S. A. Wharton, W. Weis, and D. C. Wiley.** 1988. Studies on the structure of the influenza virus hemagglutinin at the pH of membrane fusion. J. Gen. Virol. **69:**2785–2795.
27. **Ruigrok, R. W. H., S. R. Martin, S. A. Wharton, J. J. Skehel, P. M. Bayley, and D. C. Wiley.** 1986. Conformational changes in the hemagglutinin of influenza virus which accompany heat-induced fusion of virus with liposomes. Virology **155:**484–497.
28. **Sarkar, D. P., S. J. Morris, O. Eidelman, J. Zimmerberg, and R.**

Blumenthal. 1989. Initial stages of influenza hemagglutinin-induced cell fusion monitored simultaneously by two fluorescent events: cytoplasmic continuity and membrane mixing. J. Cell Biol. **109:**113–122.

29. **Sato, S. B., K. Kawasaki, and S. I. Ohnishi.** 1983. Hemolytic activity of influenza virus hemagglutinin glycoproteins activated in mildly acidic environments. Proc. Natl. Acad. Sci. USA **80:**3153–3157.
30. **Skehel, J. J., P. M. Bayley, E. B. Brown, S. R. Martin, M. D. Waterfield, J. M. White, I. A. Wilson, and D. C. J. Wiley.** 1982. Changes in the conformation of influenza virus hemagglutinin at the pH optimum of virus-mediated membrane fusion. Proc. Natl. Acad. Sci. USA **79:**968–972.
31. **Spruce, A. E., A. Iwata, and W. Almers.** 1991. The first milliseconds of the pore formed by a fusogenic viral envelope protein during membrane fusion. Proc. Natl. Acad. Sci. USA **88:**3623–3627.
32. **Spruce, A. E., A. Iwata, J. M. White, and W. Almers.** 1989. Patch clamp studies of single cell-fusion events mediated by a viral fusion protein. Nature (London) **342:**555–558.
33. **Stegmann, T., F. P. Booy, and J. Wilschut.** 1987. Effects of low pH on influenza virus. Activation and inactivation of the membrane fusion capacity of the hemagglutinin. J. Biol. Chem. **262:**17744–17749.
34. **Stegmann, T., R. W. Doms, and A. Helenius.** 1989. Protein-mediated membrane fusion. Annu. Rev. Biophys. Chem. **18:** 187–211.
35. **Stegmann, T., D. Hoekstra, G. Scherphof, and J. Wilschut.** 1986. Fusion activity of influenza virus: a comparison between biological and artificial target membrane vesicles. J. Biol. Chem. **261:**10966–10969.
36. **Stegmann, T., J. M. White, and A. Helenius.** 1990. Intermediates in influenza-induced membrane fusion. EMBO J. **9:**4231–4241.
37. **Udenfriend, S., S. Stein, P. Bohlen, W. Dairman, W. Leimgruber, and M. Weigele.** 1972. Fluorescamine: a reagent for assay of amino acids, peptides, proteins, and primary amines in the picomole range. Science **178:**871–872.
38. **Webster, R. G., L. E. Brown, and D. C. Jackson.** 1983. Changes in the antigenicity of the hemagglutinin molecule of H3 influenza virus at acidic pH. Virology **126:**587–599.
39. **Weis, W. I., A. T. Bruenger, J. J. Skehel, and D. C. Wiley.** 1990. Refinement of the influenza virus hemagglutinin by simulated annealing. J. Mol. Biol. **212:**737–761.
40. **Wharton, S. A., R. W. H. Ruigrok, S. R. Martin, J. J. Skehel, P. M. Bayley, W. Weis, and D. C. Wiley.** 1988. Conformational aspects of the acid-induced fusion mechanism of influenza virus hemagglutinin. J. Biol. Chem. **263:**4474–4480.
41. **White, J.** Unpublished observations.
42. **White, J. M.** 1990. Viral and cellular membrane fusion proteins. Annu. Rev. Physiol. **52:**675–697.
43. **White, J. M., and I. A. Wilson.** 1987. Anti-peptide antibodies detect steps in a protein conformational change: low-pH activation of the influenza virus hemagglutinin. J. Cell Biol. **105:**2887–2896.
44. **Wiley, D. C., and J. J. Skehel.** 1987. The structure and function of the hemagglutinin membrane glycoprotein of influenza virus. Annu. Rev. Biochem. **56:**365–394.
45. **Wilschut, J.** 1989. Intracellular membrane fusion. Curr. Opin. Cell Biol. **1:**639–647.
46. **Wilson, D. W., C. A. Wilcox, G. C. Flynn, E. Chen, W.-J. Kuang, W. J. Henzel, M. R. Block, A. Ullrich, and J. E. Rothman.** 1989. A fusion protein required for vesicle-mediated transport in both mammalian cells and yeast. Nature (London) **339:**355–359.
47. **Wilson, I. A., H. L. Niman, R. A. Houghten, A. R. Cherenson, M. L. Connolly, and R. A. Lerner.** 1984. The structure of an antigenic determinant in a protein. Cell **37:**767–778.
48. **Wilson, I. A., J. J. Skehel, and D. C. Wiley.** 1981. Structure of the haemagglutinin membrane glycoprotein of influenza virus at 3 A resolution. Nature (London) **289:**366–372.
49. **Yewdell, J. W., W. Gerhard, and T. Bachi.** 1983. Monoclonal anti-hemagglutinin antibodies detect irreversible antigenic alterations that coincide with the acid activation of influenza virus A/PR/834-mediated hemolysis. J. Virol. **48:**239–248.